EUROPEAN ORGANIZATION FOR NUCLEAR RESEARCH

$K^{\pm}p$ ELASTIC SCATTERING AT 3.55 GeV/c

J. Banaigs, J. Berger, C. Bonnel*), J. Duflo,
L. Goldzahl and F. Plouin

Département Saturne, Saclay, France.

W.F. Baker, P.J. Carlson, V. Chabaud and A. Lundby

CERN, Geneva, Switzerland.

ABSTRACT

We present results of measurements of $K^{\pm}p$ elastic scattering at 3.55 GeV/c in the c.m. angular ranges from 10° to 70° [$0.16 < -t < 2$ $(GeV/c)^2$] and from 100° to 170° [$3.4 < -t < 5.5$ $(GeV/c)^2$]. These results complement previously published data from this group[1]) which covered the angular region near 180°. Forward K^-p elastic scattering has a structure near $t = -1$ $(GeV/c)^2$, whilst the forward K^+p angular distribution is smooth. A backward peak is observed in the K^+p angular distribution, whilst the K^-p differential cross-section decreases towards 180°.

Geneva - 14 January 1969

(Submitted to Nuclear Physics)

*) The results presented here will be used for a doctorate thesis in physics which will be submitted by C. Bonnel at the Faculté des Sciences de Paris.

$K^{\pm}p$ ELASTIC SCATTERING AT 3.55 GeV/c

J. Banaigs, J. Berger, C. Bonnel, J. Duflo,
L. Goldzahl and F. Plouin

Département Saturne, Saclay, France.

W.F. Baker, P.J. Carlson, V. Chabaud and A. Lundby

CERN, Geneva, Switzerland.

1. INTRODUCTION

The elastic scattering of K mesons on protons has been studied previously at momenta around 3.5 GeV/c by de Baere et al.[2] for K^+p and by Gordon[3] for K^-p. Backward scattering measurements were reported by Banaigs et al.[1] for K^+p and K^-p, and by Cline et al.[4] for K^+p. In this paper we report results on K^+p and K^-p elastic scattering at 3.55 GeV/c, both in the forward and in the backward hemisphere.

The object of the experiment was to obtain a nearly complete angular distribution of $K^{\pm}p$ elastic scattering, with particular emphasis on the backward direction. Our previous publication[1] showed for the first time the backward peak in K^+p scattering, and the very small cross-section for K^-p backward scattering. In the present paper we extend these results to angles further away from 180°, and in addition we report data on forward scattering.

2. EXPERIMENTAL METHOD

In this experiment, performed at the CERN Proton Synchrotron, the elastic scattering of $K^{\pm}$ mesons on protons was measured using optical spark chambers. The experimental arrangement has been described in a previous publication[5].

The incident K mesons were identified by means of three threshold Čerenkov counters[6]. Two of them were set to record pions, and their signals were used in anticoincidence. The third Čerenkov counter was set to count kaons and pions, and was used in coincidence in the positive beam. The information from this counter was displayed on a data-box, which made it possible to measure antiproton-proton scattering in the case of the negative beam. The positive beam contained 2.7% K^+ and the negative beam 1.7% K^-. When the Čerenkov counters identified the K mesons, the pion contamination was less than 1.2% and 2.9% for K^+ and K^-, respectively. The positive beam had also a proton contamination which was less than 5%. The beam had a momentum dispersion of ±0.5% around the central value of 3.55 GeV/c which was known to ±50 MeV/c.

The forward recoil protons were momentum-analysed for large momentum transfers, whilst for small momentum transfers the scattered mesons were momentum-analysed. For $-t < 0.16$ $(GeV/c)^2$ the geometrical acceptance becomes small. A total of 127,000 spark chamber photographs were taken with an incident flux of 10^5 particles per 200 msec spill. The photographs were measured automatically by Luciole, a CRT flying-spot digitizer developed at CERN[7].

The analysis programs and the derivation of the cross-sections have been described in earlier publications[1,5,6].

3. RESULTS AND DISCUSSION

The results are given in Tables 1-3 and Figs. 1 to 5, where we have also plotted our previous data as well as results from other experiments. We have parametrized the forward angular distributions according to $d\sigma/dt = A \cdot \exp(Bt)$, and the results of the fits are given in Table 4.

Our results on forward scattering (Figs. 1 and 2) agree well with the data of de Baere et al.[2] and of Gordon[3]. It should be noticed that our improved statistical accuracy in the region near $t = -1$ $(GeV/c)^2$ makes the break, and possibly the dip, in the K^-p data stand out very clearly, whilst the K^+p data remain smooth.

Our results on backward K^+p elastic scattering are shown in Fig. 3, together with the results at lower[8] and at higher[9] momenta. The general shapes of the curves are seen to be similar. We have not sufficient statistics, however, to confirm the fast rise at positive u-values [exp (8u)] of the very accurate differential cross-sections at 2.3 GeV/c [8]. Our data in Fig. 3 are, on the other hand, in disagreement with the tentative conclusion of Cline et al.[4] that the differential cross-section turns over and decreases for positive u-values. Furthermore, the recently published data of Abrams et al.[10] at 2.76 GeV/c support our conclusion.

The final complete angular distributions are shown in Fig. 4. We notice the striking difference between the K^+p and the K^-p angular distributions, both in the forward and in the backward directions. This is in contrast to π^+p and π^-p elastic scattering at the same momentum, where the forward cross-sections almost coincide[11], and where there are backward peaks in both cases[6].

In Fig. 5 we have plotted the differential cross-sections at $u = 0$ as a function of s. They vary as s^{-4} for K^+p and s^{-10} for K^-p.

The backward K^-p angular distributions in the region from 1 to 2.5 GeV/c[8] indicate that the contribution of the resonance formation mechanism saturates the cross-sections. This contribution is found to decrease very rapidly with energy, in agreement with our cross-section limit at 3.55 GeV/c (Figs. 4 and 5). On the other hand, the K^+p data show no clear indication of resonances[12]. We therefore conclude that the dominating mechanisms at our energy are i) diffraction (Pomeron exchange) and meson exchange for forward K^+p scattering, and ii) baryon exchange for backward K^+p scattering[13]. As regards backward K^-p scattering, the smallness of the cross-section is ascribed to the lack of an $S = +1$ baryon to be exchanged, and to the weaker contribution of two- (or more)-particle exchange mechanism (cuts)[*].

Meson or baryon exchange contributions decrease rapidly with energy and must be quite different for K^+p and for K^-p. This can be understood in terms of the finite energy sum rules[15] that relate the Regge parameters of the high-energy data to the low-energy measurements. From the discussion in the preceding paragraph, one should therefore expect a different behaviour of the K^+p and K^-p data as one goes to higher energy. This has been further emphasized by Schmid[16], who showed that partial wave projections of the phase factor $1 \pm e^{-i\pi\alpha}$ in the Regge amplitude lead to resonances unless the term $e^{-i\pi\alpha}$ is cancelled. Such a cancellation should occur, and does in fact occur for both forward and backward K^+p scattering for which the relevant meson and hyperon trajectories appear in exchange-degenerate pairs of opposite signature[16].

---

*) According to Chiu and Finkelstein[14] the energy-dependence of a Regge cut contribution should be $s^{[2(\alpha_1 + \alpha_2) - 4]}/\ln(s/s_0)^2$, where α_1 and α_2 are the trajectories exchanged. In the case of K^-p backward scattering the exchanged trajectories would probably be K^* and N, which would at most give s^{-6}.

We have analysed backward K^+p scattering in these terms. According to Schmid, the dominant trajectories are $\Lambda_\alpha(1115, 1815)$ and $\Lambda_\gamma(1520, 2100)$. From Fig. 6, exchange degeneracy is evident for the trajectories:

$$\alpha_{\Lambda_\gamma}(\sqrt{u}) = \alpha_{\Lambda_\alpha}(\sqrt{u}) \ .$$

Furthermore, Schmid has shown that exchange degeneracy applies also to the residue functions:

$$\beta_{\Lambda_\gamma}(\sqrt{u}) \simeq \beta_{\Lambda_\alpha}(\sqrt{u}) \ .$$

If we drop kinematical factors, the contribution of either Λ_α or Λ_γ to the Regge amplitude is

$$R \propto \left(\frac{s}{s_0}\right)^{\alpha(\sqrt{u})-\frac{1}{2}} \frac{\beta(\sqrt{u})}{\Gamma[\alpha(\sqrt{u}) + \frac{1}{2})]} \frac{1 \pm i\ e^{-i\pi\alpha(\sqrt{u})}}{\cos \pi\alpha(\sqrt{u})}$$

where the signature is + for Λ_α and - for Λ_γ.

The total amplitude is therefore:

$$R(\Lambda_\alpha) + R(\Lambda_\gamma) \propto \left(\frac{s}{s_0}\right)^{\alpha(\sqrt{u})-\frac{1}{2}} \frac{2\ \beta(\sqrt{u})}{\Gamma[\alpha(\sqrt{u}) + \frac{1}{2}]\ \cos \pi\ \alpha(\sqrt{u})} \ .$$

The first conclusion we can draw is that the cancellation of the term $e^{-i\pi\alpha}$ has removed the zero in R which would have occurred at $\alpha_{\Lambda_\alpha} = -\frac{1}{2}$ or $\alpha_{\Lambda_\gamma} = -\frac{3}{2}$, if Λ_α or Λ_γ contributed alone. According to Fig. 6, with Λ_α alone we would have expected the K^+p backward angular distribution to have a dip for positive u values, analogous to the dip at $u = -0.15\ (\mathrm{GeV}/c)^2$ for π^+p scattering. Complete exchange degeneracy of the residue functions and trajectories of the Λ_α and Λ_γ poles has removed this dip in agreement with the results in Figs. 3 and 4.

Secondly, in Fig. 6 we notice that the intercept of the Λ_α and Λ_γ trajectories at $u = 0$ is $\alpha \simeq -0.7$. This gives the s-dependence of the differential cross-section $(d\sigma/du)_{u=0} \propto s^{-3.4}$ in agreement with Fig. 5.

The fits to the angular distributions in Fig. 3 have been obtained by using the complete expressions for the Regge amplitudes f_1 and f_2 given by Chiu and Stack[17], and with the following assumptions for the trajectories and residue functions:

$$\alpha_{\Lambda_\alpha} = \alpha_{\Lambda_\gamma} = -0.70 + 0.95\ u$$

$$\beta_{\Lambda_\alpha} = \beta_0 \left(1 - \frac{\sqrt{u}}{1.115}\right)$$

$$\beta_{\Lambda_\gamma} = \beta_0 \left(1 - \frac{\sqrt{u}}{1.52}\right) .$$

The two terms in brackets have been introduced to take into account the non-existence of the MacDowell symmetric states $\Lambda_\beta(1115)$ and $\Lambda_\delta(1520)$. The only free parameter in the fit is β_0, and we found

$$\beta_0 = -10\ \mathrm{GeV}^{-1} .$$

If we extrapolate the fitted residue functions to the positions of the first physical states on the Λ_α and Λ_γ trajectories, we find a coupling constant $g^2_{KN\Lambda}/4\pi = 3$ instead of 16 [18] for $\Lambda_\alpha(1115)$, and an elastic width $\Gamma_{el} \simeq 2$ MeV instead of 7 MeV [19] for $\Lambda_\gamma(1520)$. When looking at the fits in Fig. 3 it should be kept in mind that there is a background due to a tail of the forward scattering amplitude in the backward hemisphere, which may be of the order of 1% at 3.55 GeV/c and 10% at 2.3 GeV/c (Fig. 4).

Turning now to forward scattering, we notice a structure for K^-p at $t = -1\ (\mathrm{GeV}/c)^2$, whilst K^+p shows a smooth behaviour. The structure in K^-p diminishes with energy [20] and is therefore associated with the finite energy contributions (meson exchange). There is therefore no evidence for a structure in asymptotic $K^\pm p$ scattering like there is in asymptotic pp scattering [21]. The data are not accurate enough to show such a structure, if it existed, for $|t| > 1.5\ (\mathrm{GeV}/c)^2$. The finite energy contributions may be sufficient to smooth out a possible structure at our momentum, or the K meson may be sufficiently smaller than the proton and therefore lead to a structure at larger momentum transfers.

A fit has been reported by Blackmon and Goldstein [22] to the very forward $K^\pm p$ elastic scattering using meson and Pomeron exchanges in an eikonal model.

Table 1

K^+p elastic differential cross-sections at 3.55 GeV/c in the forward direction. Listed errors are statistical. There is an over-all uncertainty of scale of ±15%. s=7.85 $(GeV)^2$, $p^{c.m.}$ = 1.19 GeV/c.

cos $\Theta_K^{c.m.}$	-t $(GeV/c)^2$	Δt $(GeV/c)^2$	No. of events	$d\sigma/dt$ mb/$(GeV/c)^2$	$d\sigma/d\Omega$ mb/sr
0.9363	0.18	0.04	697	9.20 ± 0.35	4.14 ± 0.16
0.9186	0.23	0.06	859	8.10 ± 0.28	3.64 ± 0.12
0.8974	0.29	0.06	626	6.46 ± 0.26	2.91 ± 0.12
0.8762	0.35	0.06	493	5.30 ± 0.24	2.39 ± 0.11
0.8550	0.41	0.06	361	4.10 ± 0.22	1.84 ± 0.10
0.8337	0.47	0.06	266	3.20 ± 0.20	1.44 ± 0.09
0.8125	0.53	0.06	178	2.32 ± 0.17	1.05 ± 0.08
0.7913	0.59	0.06	142	2.01 ± 0.17	0.90 ± 0.08
0.7700	0.65	0.06	110	1.69 ± 0.16	0.76 ± 0.07
0.7488	0.71	0.06	83	1.37 ± 0.15	0.62 ± 0.07
0.7205	0.79	0.06	93	1.03 ± 0.10	0.47 ± 0.05
0.6851	0.89	0.10	52	0.63 ± 0.09	0.29 ± 0.04
0.6498	0.99	0.10	35	0.58 ± 0.10	0.26 ± 0.04
0.6144	1.09	0.10	24	0.43 ± 0.09	0.19 ± 0.04
0.5613	1.24	0.20	19	0.17 ± 0.04	0.07 ± 0.02
0.4552	1.54	0.40	9	0.05 ± 0.02	0.02 ± 0.01

Table 2

K^-p elastic differential cross-sections at 3.55 GeV/c in the forward direction. Listed errors are statistical. There is an over-all uncertainty of scale of ±15%. $s=7.85$ $(GeV)^2$, $p^{c.m.} = 1.19$ GeV/c.

$\cos\Theta_K^{c.m.}$	$-t$ $(GeV/c)^2$	Δt $(GeV/c)^2$	No. of events	$d\sigma/dt$ mb/(GeV/c)	$d\sigma/d\Omega$ mb/sr
0.9328	0.19	0.06	223	7.45 ± 0.50	3.35 ± 0.22
0.9116	0.25	0.06	150	5.34 ± 0.44	2.40 ± 0.20
0.8903	0.31	0.06	68	2.75 ± 0.33	1.24 ± 0.15
0.8585	0.40	0.12	73	1.55 ± 0.18	0.69 ± 0.08
0.8160	0.52	0.12	66	0.65 ± 0.08	0.29 ± 0.04
0.7736	0.64	0.12	38	0.35 ± 0.06	0.16 ± 0.03
0.7241	0.78	0.16	27	0.19 ± 0.04	0.09 ± 0.02
0.6604	0.96	0.20	11	0.12 ± 0.04	0.05 ± 0.02
0.5896	1.16	0.20	7	0.07 ± 0.03	0.03 ± 0.01
0.5189	1.36	0.20	7	0.09 ± 0.03	0.04 ± 0.02
0.4481	1.56	0.20	7	0.13 ± 0.05	0.06 ± 0.02
0.3420	1.86	0.40	3	0.04 ± 0.02	0.02 ± 0.01

Table 3

$K^{\pm}p$ elastic differential cross-sections at 3.55 GeV/c in the backward direction. Listed errors are statistical. There is an over-all uncertainty of scale of ±15%

Particle	$\cos\Theta_K^{c.m.}$	u $(GeV/c)^2$	Δu $(GeV/c)^2$	No. of events	$d\sigma/du$ mb/$(GeV/c)^2$	$d\sigma/d\Omega$ mb/sr
K^+	-0.9940	0.035	0.023	15*)	47.4 ± 13.1	21.3 ± 5.9
	-0.9835	0.005	0.037	7*)	33.1 ± 12.9	14.9 ± 5.8
	-0.9358	-0.130	0.100	7	20.2 ± 7.7	9.1 ± 3.5
	-0.9004	-0.230	0.100	7	19.3 ± 6.9	8.7 ± 3.1
	-0.8473	-0.380	0.200	6	10.2 ± 4.2	4.6 ± 1.9
	-0.7589	-0.630	0.300	6	8.0 ± 3.5	3.6 ± 1.6
	-0.6351	-0.980	0.400	6	9.6 ± 4.2	4.3 ± 1.9
	-0.4546	-1.490	0.600	5	7.4 ± 3.5	3.3 ± 1.6
K^-	-0.9875	0.016	0.060	0	< 3.2	< 1.4
	-0.6280	-1.000	2.000	3	3.2 ± 1.9	1.5 ± 0.8

*) These events very close to 180° were obtained in another geometry (Ref. 1)

Table 4

Results of a least squares fit to the forward diffraction peak to the form $d\sigma/dt = Ae^{Bt}$

Particle	Range in $-t$ $(\mathrm{GeV}/c)^2$	A $\mathrm{mb}/(\mathrm{GeV}/c)^2$	B $(\mathrm{GeV}/c)^{-2}$	$P(\chi^2 > \chi^2_{obs.})$
K^+ *)	0.16 - 1.74	18.5 ± 0.6	3.69 ± 0.08	0.8
K^-	0.16 - 0.58	32.0 ± 3.7	7.53 ± 0.38	0.5

*) The proton contamination in our K^+ beam is less than 5%. Assuming this contamination and subtracting the corresponding pp differential cross-sections we get $A = (15.3 \pm 0.6)\ \mathrm{mb}/(\mathrm{GeV}/c)^2$ and $B = (3.47 \pm 0.09)\ (\mathrm{GeV}/c)^{-2}$.

REFERENCES

1) J. Banaigs, J. Berger, C. Bonnel, J. Duflo, L. Goldzahl, F. Plouin, W.F. Baker, P.J. Carlson, V. Chabaud and A. Lundby, Phys. Letters 24 B, 317 (1967).

2) W. De Baere, J. Debaisieux, P. Dufour, F. Grard, J. Heughebaert, L. Pape, P. Peeters, F. Verbeure, R. Windmolders, R. George, Y. Goldschmidt-Clermont, V.P. Henri, B. Jongejans, D.W.G. Leith, A. Moisseev, F. Muller, J.M. Perreau and V. Yarba, Nuovo Cimento 45 A, 885 (1966).

3) J. Gordon, Phys. Letters 21, 117 (1966). The K^- beam had a π^- contamination of 11 ± 5%.

4) D. Cline, C. Moore and D. Reeder, Phys.Rev.Letters 19, 675 (1967).

5) J. Banaigs, J. Berger, C. Bonnel, J. Duflo, L. Goldzahl, F. Plouin, W.F. Baker, P.J. Carlson, V. Chabaud and A. Lundby, Nuclear Physics B8, 31 (1968).

6) W.F. Baker, P.J. Carlson, V. Chabaud, A. Lundby, E.G. Michaelis, J. Banaigs, J. Berger, C. Bonnel, J. Duflo, L. Goldzahl and F. Plouin, Nuclear Physics (in press).

7) H. Anders, T. Lingjaerde and D. Wiskott, Proc.Int.Symposium on Nuclear Electronics, Paris (1963), p. 349.
A.E. Head and J.A. Wilson, Proc.Conf. on Programming for Flying-Spot Devices, Bologna (1964), CERN Report 65-11 (1965), p.57.
T.F. Andersson, P.M. Blackhall, J. Daub, A.E. Head, M.B. Metcalf and V.J. Weights, Proc.Int.Conf. on Programming for Flying-Spot Devices, Munich (1967), p. 86.

8) A.S. Carroll, J. Fischer, A. Lundby, R.H. Phillips, C.L. Wang, F. Lobkowicz, A.C. Melissinos, Y. Nagashima and S. Tewksbury, Phys.Rev. Letters 21, 1282 (1968); University of Rochester Rep. 875-254 (1968).

9) W.F. Baker, K. Berkelman, P.J. Carlson, G.P. Fisher, P. Fleury, D. Hartill, R. Kalbach, A. Lundby, S. Mukhin, R. Nierhaus, K.P. Pretzl and J. Woulds, Phys. Letters 28B, 292 (1968).

10) G.S. Abrams, L. Eisenstein, T.A. O'Halloran, Jr., W. Shufeldt and J. Whitmore, Phys.Rev. Letters 21, 1407 (1968).

11) C. Coffin, N. Dikmen, L. Ettlinger, D. Meyer, A. Saulys, K. Terwilliger and D. Williams, Phys.Rev. Letters 15, 838 (1965) and 17, 458 (1966).

12) See review paper by R. Tripp, Strange baryon resonances, Proc. 14th Int. Conf. on High-Energy Physics (1968), p. 173.

13) For a review, see Chan Hong-Mo, Advances in the theory of collisions at high energy, Proc. 14th Int. Conf. on High-Energy Physics, Vienna (1968) (CERN, Geneva, 1968), p. 391.

14) C.B. Chiu and J. Finkelstein, CERN TH. 914 (1968).

15) R. Dolen, D. Horn and C. Schmid, Phys.Rev. 166, 1768 (1968).

16) C. Schmid, Phys.Rev.Letters 20, 689 (1968).
C. Schmid, CERN TH. 960 (1968).

17) C.B. Chiu and J.D. Stack, Phys.Rev. 153, 1575 (1967).

18) J.K. Kim, Phys.Rev. Letters 19, 1079 (1967).

19) N. Barash-Schmidt, A. Barbaro-Galtieri, L.R. Price, M. Roos, A.H. Rosenfeld, P. Söding and C.G. Wohl, UCRL-8030, Aug. 1968.

20) J. Orear, D.P. Owen, C.F. Peterson, A.L. Read, D.G. Ryan, D.H. White, A. Ashmore, C.J. Damerell, W.R. Frisken and R. Rubinstein, Phys. Letters 28 B, 61 (1968).

21) J.V. Allaby, A.N. Diddens, A. Klovning, E. Lillethun, E.J. Sacharidis, K. Schlüpmann and A.M. Wetherell, Proc. of the Topical Conf. on the High-Energy Collisions of Hadrons, CERN (1968), CERN 68-7, p. 580.

22) M.L. Blackmon and G.R. Goldstein, ANL/HEP 6819 (1968).

Figure captions

Fig. 1 : K^+p forward elastic scattering at 3.55 GeV/c measured in this experiment. Also shown are data from W. De Baere et al.[2].

Fig. 2 : K^-p forward elastic scattering at 3.55 GeV/c measured in this experiment. Also shown are data from Gordon[3].

Fig. 3 : K^+p backward elastic scattering. The data at 2.33 GeV/c are from BNL-Rochester[8]; at 3.55 GeV/c, this experiment; at 5.2 and 6.9 GeV/c, from CERN[9]. The solid lines are the Regge-pole fits discussed in the text.

Fig. 4 : Complete angular distribution of $K^{\pm}p$ elastic scattering at 3.55 GeV/c. The data points are from this experiment and from that of W. De Baere et al.[2]. The solid lines are drawn to guide the eye.

Fig. 5 : K^+p elastic differential cross-section at u=0 as a function of s. The data are from BNL-Rochester[8], CERN[9], and this experiment.

Fig. 6 : Chew-Frautschi plot of the exchange-degenerate Λ_α and Λ_γ trajectories believed to be responsible for K^+p backward scattering.

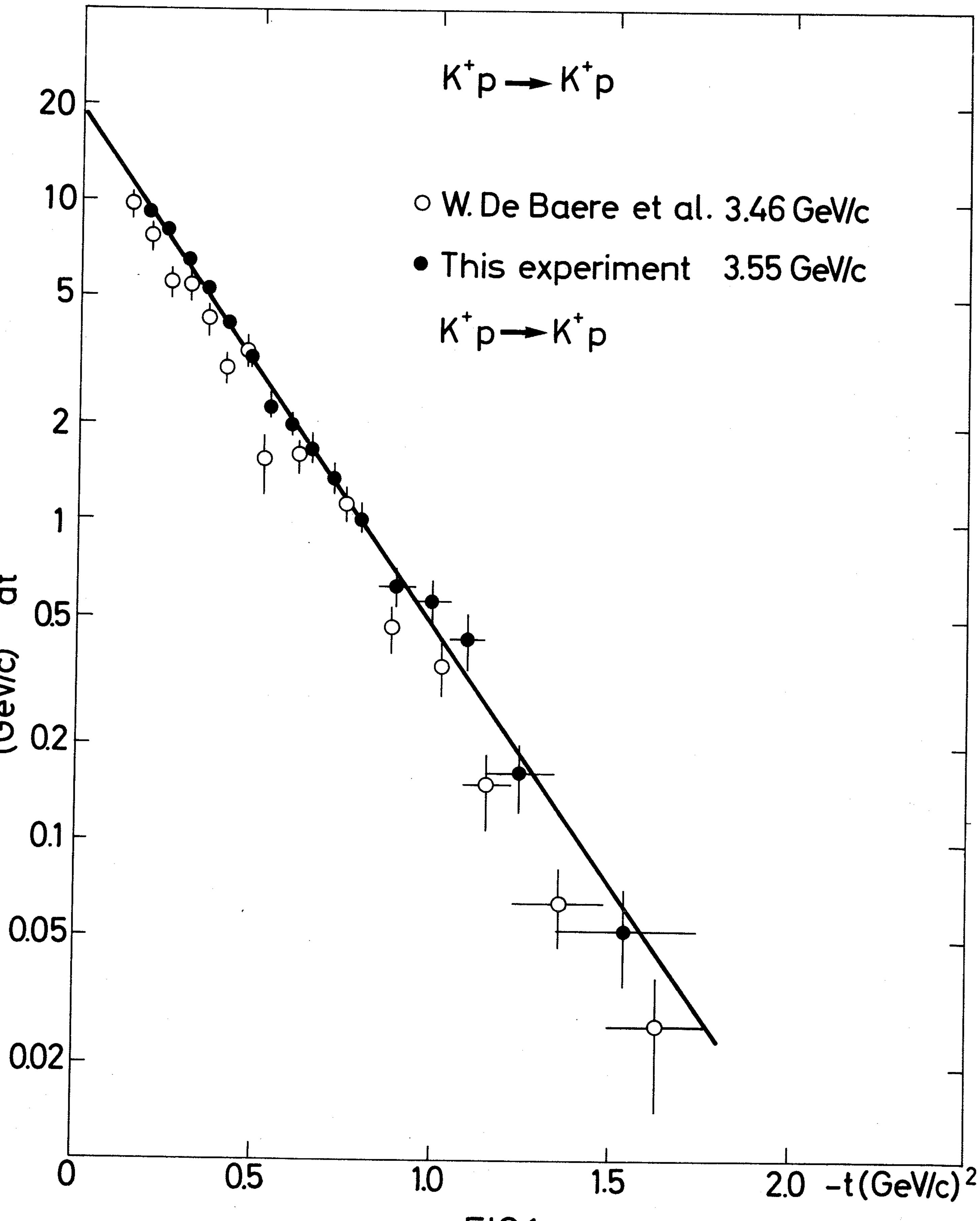

K⁺p → K⁺p
○ W. De Baere et al. 3.46 GeV/c
● This experiment 3.55 GeV/c
K⁺p → K⁺p
20
10
5
2
1
0.5
0.2
0.1
0.05
0.02
mb/(GeV/c)² dσ/dt
0
0.5
1.0
1.5
2.0
-t (GeV/c)²

FIG.1

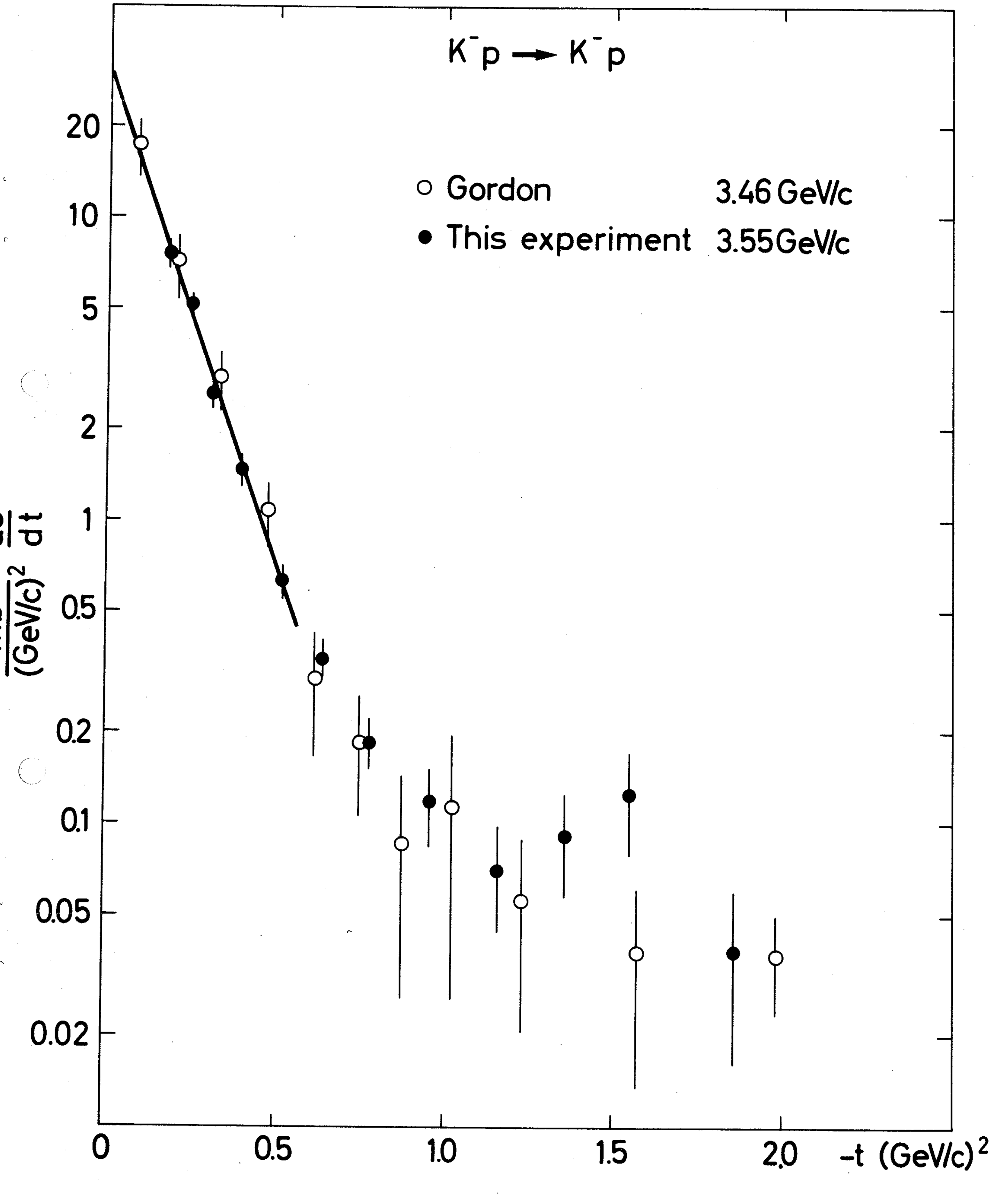
$K^-p \rightarrow K^-p$
○ Gordon 3.46 GeV/c
● This experiment 3.55 GeV/c
20
10
5
2
1
0.5
0.2
0.1
0.05
0.02
0
0.5
1.0
1.5
2.0
$-t\ (\mathrm{GeV/c})^2$
$\frac{\mathrm{mb}}{(\mathrm{GeV/c})^2}\ \frac{d\sigma}{dt}$

FIG. 2

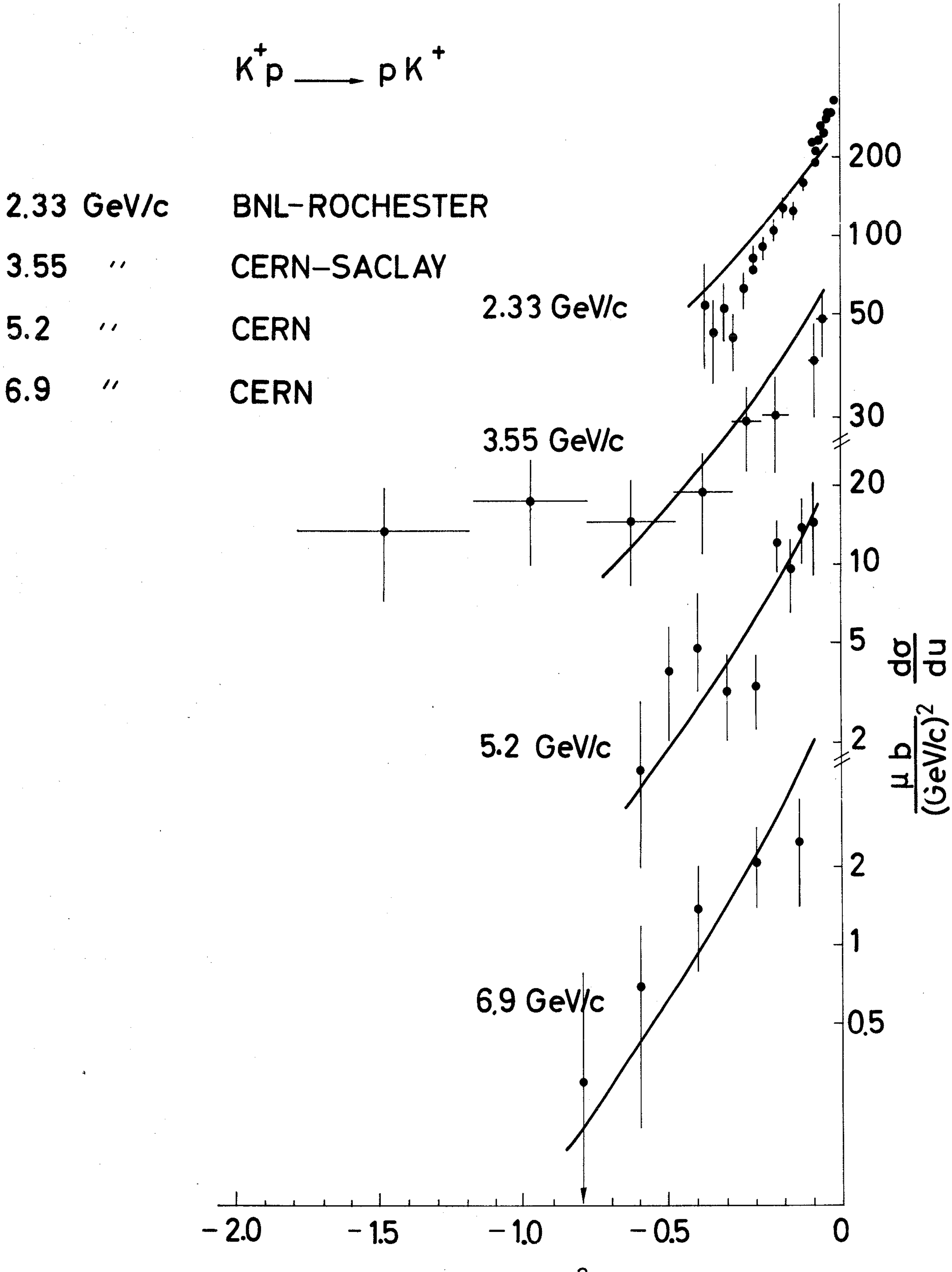

K⁺p ⟶ pK⁺
2.33 GeV/c BNL-ROCHESTER
3.55 ″ CERN-SACLAY
5.2 ″ CERN
6.9 ″ CERN
2.33 GeV/c
3.55 GeV/c
5.2 GeV/c
6.9 GeV/c
200
100
50
30
20
10
5
2
2
1
0.5
μb/(GeV/c)² dσ/du
-2.0
-1.5
-1.0
-0.5
0
u (GeV/c)²

FIG.3

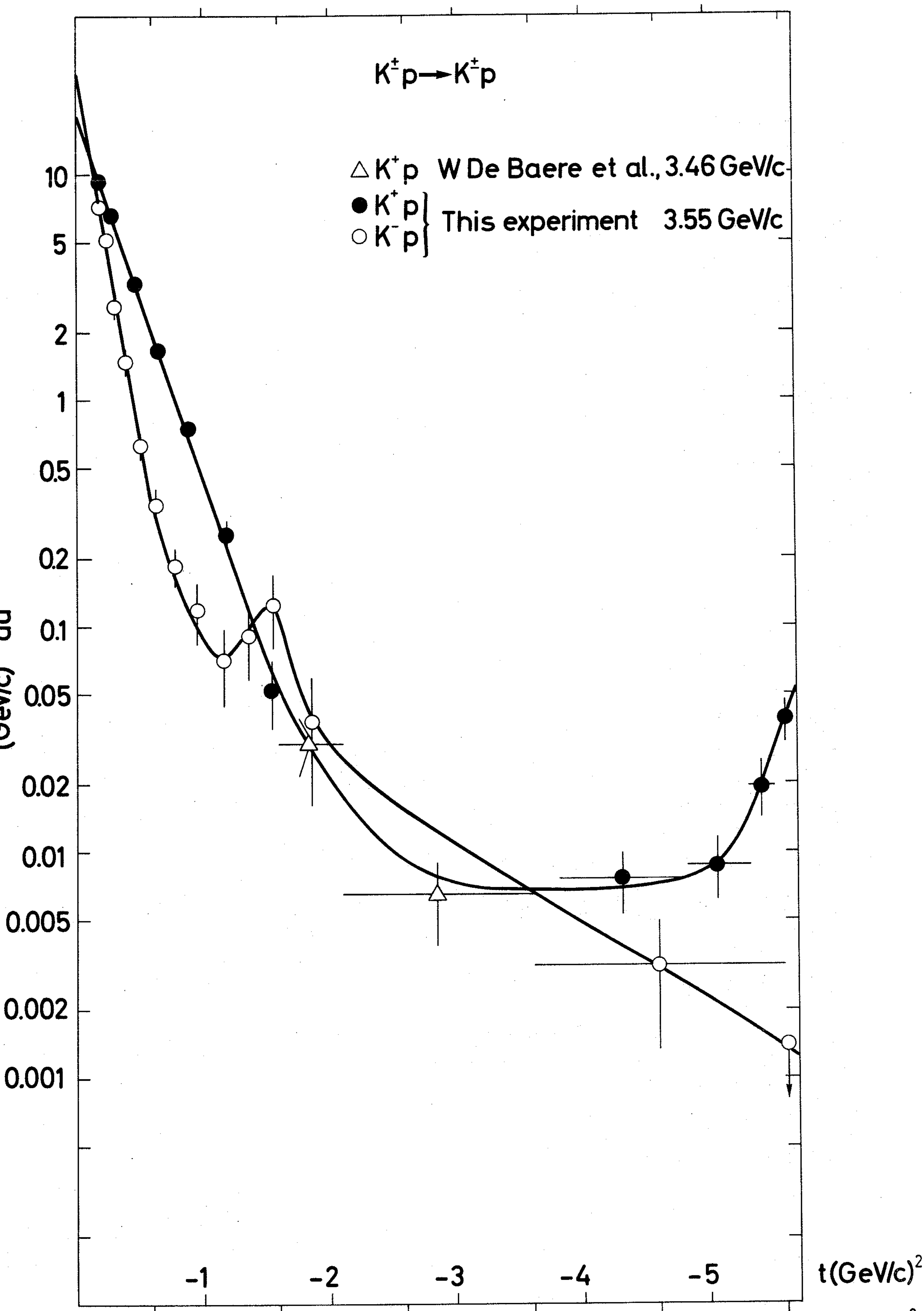

K±p → K±p
△ K⁺p W De Baere et al., 3.46 GeV/c
● K⁺p
○ K⁻p
This experiment 3.55 GeV/c
10
5
2
1
0.5
0.2
0.1
0.05
0.02
0.01
0.005
0.002
0.001
mb/(GeV/c)² dσ/du
-1
-2
-3
-4
-5
t(GeV/c)²
-5
-4
-3
-2
-1
0 u(GeV/c)²

FIG.4

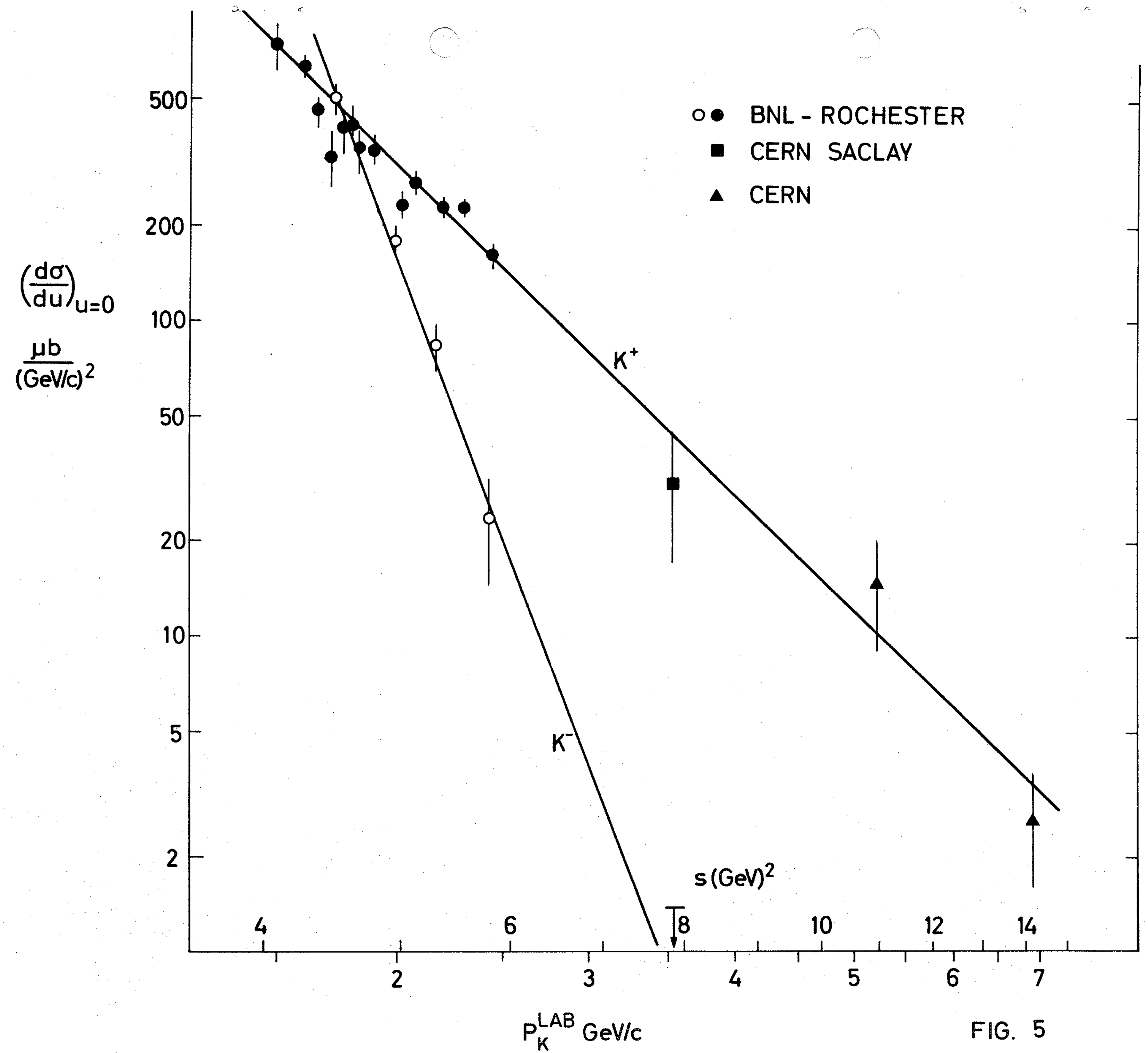
BNL - ROCHESTER
CERN SACLAY
CERN
K+
K-
500
200
100
50
20
10
5
2
s (GeV)2
4
6
8
10
12
14
2
3
4
5
6
7
$\left(\frac{d\sigma}{du}\right)_{u=0}$
$\frac{\mu b}{(GeV/c)^2}$
P_K^{LAB} GeV/c

FIG. 5

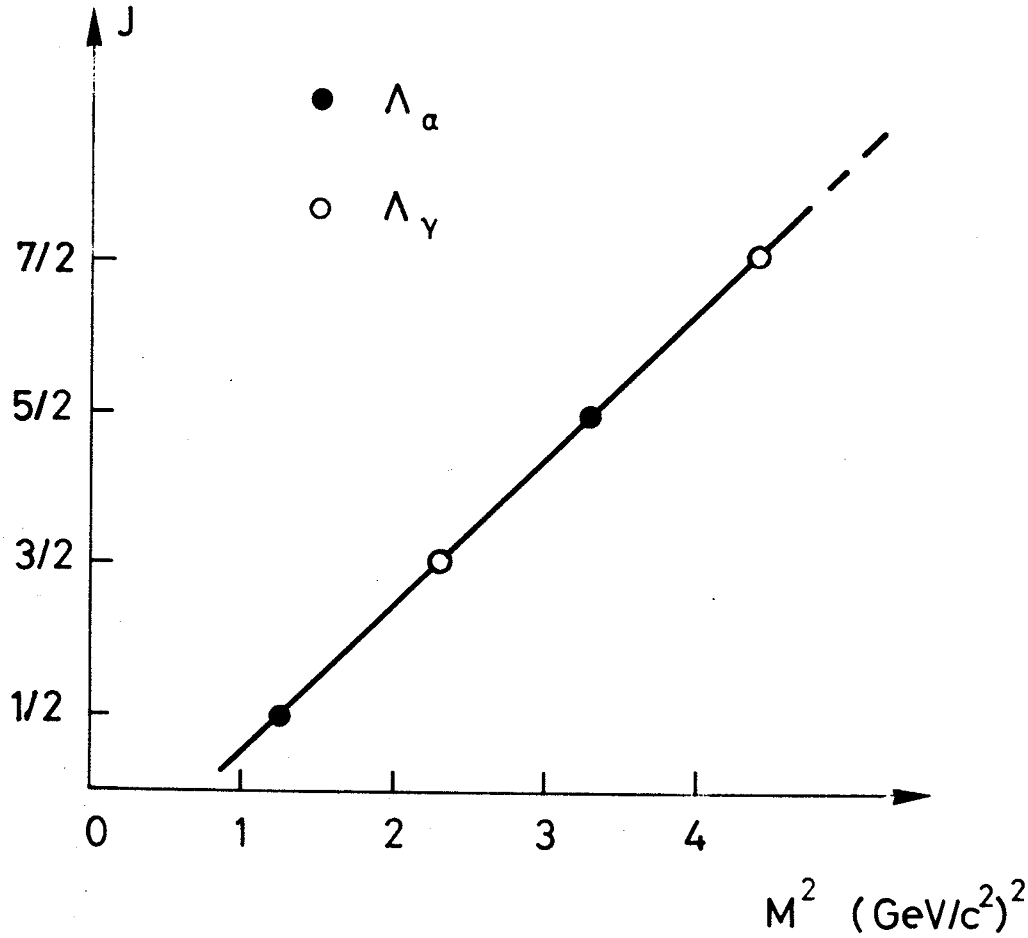

FIG . 6